ANL-7855

THE NUMERICAL SOLUTION OF THE ORR-SOMMERFELD EQUATION AT LARGE REYNOLDS NUMBER

Thomas H. Hughes

ARGONNE NATIONAL LABORATORY, ARGONNE, ILLINOIS

The facilities of Argonne National Laboratory are owned by the United States Government. Under the terms of a contract (W-31-109-Eng-38) between the U. S. Atomic Energy Commission, Argonne Universities Association and The University of Chicago, the University employs the staff and operates the Laboratory in accordance with policies and programs formulated, approved and reviewed by the Association.

MEMBERS OF ARGONNE UNIVERSITIES ASSOCIATION

The University of Arizona
Carnegie-Mellon University
Case Western Reserve University
The University of Chicago
University of Cincinnati
Illinois Institute of Technology
University of Illinois
Indiana University
Iowa State University
The University of Iowa
Kansas State University
The University of Kansas
Loyola University
Marquette University
Michigan State University
The University of Michigan
University of Minnesota
University of Missouri
Northwestern University
University of Notre Dame
The Ohio State University
Ohio University
The Pennsylvania State University
Purdue University
Saint Louis University
Southern Illinois University
The University of Texas at Austin
Washington University
Wayne State University
The University of Wisconsin

Printed in the United States of America
Available from
National Technical Information Service
U.S. Department of Commerce
5285 Port Royal Road
Springfield, Virginia 22151
Price: Printed Copy $3.00; Microfiche $0.95

ANL-7855
Mathematics and Computers

ARGONNE NATIONAL LABORATORY
9700 South Cass Avenue
Argonne, Illinois 60439

THE NUMERICAL SOLUTION OF THE ORR-SOMMERFELD EQUATION AT LARGE REYNOLDS NUMBER

by

Thomas H. Hughes

Applied Mathematics Division

September 1971

TABLE OF CONTENTS

LIST OF FIGURES

THE NUMERICAL SOLUTION OF THE ORR-SOMMERFELD EQUATION AT LARGE REYNOLDS NUMBER

by

Thomas H. Hughes

ABSTRACT

The use of an automatically-determined variable mesh in the numerical solution of the Orr-Sommerfeld equation is explored for plane Poiseuille flow. The usual finite-difference matrix method with a modified eigenvalue-search-procedure is used. The method is applicable at both small and very large Reynolds numbers and is used to piece together existing numerical and asymptotic results. The curve of neutral stability and several eigenfunctions are presented for plane Poiseuille flow. It is also demonstrated that the kink in the neutral curve is a feature of the Orr-Sommerfeld equation and not just a deficiency in the asymptotic methods as previously suggested.

I. INTRODUCTION

The Orr-Sommerfeld equation with its associated boundary conditions is a two-point boundary-value problem that has its origin in the linear theory of hydrodynamic stability. It has been observed experimentally that laminar flow occurs at low Reynolds number and that turbulent flow is the more natural flow regime for the same situation at higher Reynolds number. Since unavoidable irregularities and vibrations occur in any real flow situation, such disturbances to the basic flow must die out if a laminar flow is to remain laminar. However, the laminar regime is said to be unstable when such disturbances are observed to amplify. Linear hydrodynamic stability theory attempts to understand the decay and growth of infinitesimal disturbances as they effect the early stages of transition from laminar to turbulent flow. In the mathematical theory a given idealized steady-state solution of the equations of motion is considered and the individual Fourier components of a disturbance are studied.

The Orr-Sommerfeld equation governs the two-dimensional disturbances of parallel steady two-dimensional flows given by a velocity field $\underset{\rightarrow}{u} = \{U(y),0\}$ where the x direction is in the direction of flow and the y direction is chosen perpendicular to the flow. These flows include certain boundary layers, wakes, jets and flows between parallel planes. In this report only plane Poiseuille flow will be considered although it should not be difficult to extend the numerical method to boundary layers and shear layers. In the case of plane Poiseuille flow between stationary parallel plates, the velocity profile is

$$U(y) = 1 - y^2 \tag{1}$$

where the problem has been normalized such that the plates are located at $y = +1$ and $y = -1$, and the maximum velocity at $y = 0$ is unity.

Consider a two-dimensional disturbance to this basic flow with velocity components $\{u',v'\}$ and take a single complex Fourier component

$$\{u',v'\} = \text{Real}\{[\hat{u}(y),\hat{v}(y)]\text{Exp}[i\alpha(x-ct)]\}.$$

The quantity α is real and is the wave number in the x direction; c is complex, the real part, c_r, is the wave velocity and the imaginary part of c, namely c_i, represents the amplification or damping of the oscillation with the passage of time. The disturbance velocities u' and v' are both required to vanish at the boundaries $y = +1$ and -1. In order to derive the disturbance differential equations the perturbed velocity field $\underset{\rightarrow}{u} = \{U+u',v'\}$ is substituted into the Navier-Stokes equations and then the disturbance equations are linearized. It is convenient to define a stream function in the form

$$\psi = \phi(y)\text{Exp}[i\alpha(x-ct)]$$

where $\hat{u} = \phi'$, $\hat{v} = -i\alpha\phi$ and (') now denotes differentiation with respect to y. Then the differential equation to be satisfied by the complex function $\phi(y)$ is the Orr-Sommerfeld equation:

$$(U-c)(\phi''-\alpha^2\phi) - U''\phi = \frac{1}{i\alpha R}(\phi^{iv} - 2\alpha^2\phi'' + \alpha^4\phi) \tag{2}$$

where R is the Reynolds number. The boundary conditions are $\phi = \phi' = 0$ at $y = +1$ and $y = -1$. For plane Poiseuille flow $U(y) = 1 - y^2$ is an even function so that ϕ may be split into odd and even solutions. Only the even solution will be studied here, and therefore, only the half-channel $y = -1$ to $y = 0$ need be considered. The boundary conditions are

$$\phi = \phi' = 0 \text{ at } y = -1 \text{ and } \phi' = \phi''' = 0 \text{ at } y = 0. \tag{3}$$

The mathematical problem of hydrodynamic stability now becomes an eigenvalue problem of Eq. (2) with the boundary conditions (3) and yields an eigenrelation between α, R, c_r, and c_i. In general this eigenvalue problem is very difficult to solve. If c_i is positive, the flow is said to be unstable according to linearized theory; otherwise the flow is stable. If one considers the neutral disturbances, $c_i = 0$, the result of plotting α against R is called the 'neutral' curve, or the curve of neutral stability (see Fig. 1). Of particular interest is the lowest Reynolds number for which all disturbances are stable. From previous work[1] the range of the parameters along the neutral curve are known as follows:

R is real, $R_{min} \cong 5000$ and $R \to \infty$;

α is real, >0, with $\alpha_{max} \cong 1.5$ and $\alpha \to 0$ as $R \to \infty$;

$(c_r)_{max} \cong \frac{1}{4}$ and $c_r \to 0$ as $R \to \infty$.

II. REVIEW OF PREVIOUS WORK

Early studies of the Orr-Sommerfeld equation were based upon the fact that the Reynolds number is usually fairly large and consequently asymptotic methods were used. More recently numerical methods have been used extensively. There are two different numerical approaches: (i) the initial-value (or shooting) method in which the two-point boundary-value problem is solved by an initial-value numerical integration, and (ii) the matrix finite-difference method in which the differential equation is approximated by a finite-difference equation and then the resulting matrix eigenvalue problem is solved. The method to be presented in this report is a modification of the matrix finite-difference method. In addition the calculations by this new method are made more efficient by using some elements of the asymptotic analysis. Consequently, both asymptotic and numerical methods are reviewed in the following paragraphs.

Asymptotic Methods

The Orr-Sommerfeld equation (2) is a fourth-order linear equation; the solution therefore consists of a linear combination of four basic solutions and may be written $\phi = c_1\phi_1 + c_2\phi_2 + c_3\phi_3 + c_4\phi_4$. As a starting point in the asymptotic analysis, it is natural to expand in powers of $(i\alpha R)^{-1}$. The zeroth-order solutions of such an expansion are the so-called inviscid solutions, ϕ_1 and ϕ_2, which satisfy the differential equation

$$(U-c)(\phi''-\alpha^2\phi) - U''\phi = 0. \tag{4}$$

Consider the case $c_i = 0$. Since it is known that the value of c_r is such that $U(y) - c_r$ has a zero in the range $-1 \leq y \leq 0$, equation (4) has a singularity at $y = y_c$ where $y_c = -\sqrt{1-c_r}$. Thus equation (4) is not a valid approximation everywhere to the full Orr-Sommerfeld equation (2) which is regular at the 'critical point' y_c. Also the

solutions to (4) cannot satisfy all the boundary conditions (3), since (4) is only a second-order differential equation. Nevertheless these inviscid solutions are correct except in the neighborhood of y_c and at the wall $y = -1$. The other two basic solutions, ϕ_3 and ϕ_4, are corrections to the inviscid solutions and are known as viscous solutions. The viscous solution ϕ_3 decreases exponentially with distance from the wall and is the one which is physically realistic, while the other ϕ_4 increases exponentially with distance from the wall and must be rejected. Much of the difficulty of linear hydrodynamic stability theory is concerned with the details of providing these necessary corrections. For detailed information concerning the asymptotic work the reader is referred to the book by Lin[1] and the review articles by Stuart,[2] Shen,[3] and Reid.[4]

Initial-Value (Shooting) Methods

There are several variations to this method and the following discussion illustrates the basic idea. Choose a particular value of R (with $c_i = 0$) and estimate α and c_r. Using a numerical integration scheme such as Runge-Kutta, integrate the Orr-Sommerfeld equation from $y = 0$ to $y = -1$ to get two independent solutions ϕ_a and ϕ_b. To initiate the integration the initial values are chosen to satisfy $\phi'(0) = \phi'''(0) = 0$ and $\phi_a = 1$, $\phi_a'' = 0$, $\phi_b = 0$ and $\phi_b'' = 1$. One of the solutions will be an inviscid solution and the other of exponential type. Now apply the boundary conditions at $y = -1$ to $\phi = A\phi_a + \phi_b$. That is, $A\phi_a(-1) + \phi_b(-1) = 0$ and $A\phi_a'(-1) + \phi_b'(-1) = 0$. These equations will be satisfied if the characteristic equation $\phi_a(-1)\phi_b'(-1) - \phi_a'(-1)\phi_b(-1) = 0$ is satisfied. Since ϕ is complex there are two real equations for α and c_r that can be solved iteratively using a rootfinder such as Newton's.

The difficulty with the above method is that one of the solutions to the differential equation grows exponentially. Hence the real problem is to generate numerically a second (inviscid) solution which is not merely a multiple of the growing solution. At relatively low Reynolds numbers near R_{min}, Nachtsheim[5] overcame this difficuty by using double precision arithmetic, integrating from both $y = 0$ and $y = -1$, and

matching in the middle. Supression of the growing solution during the calculation of the well-behaved solution also overcomes this difficulty and has been used quite successfully with several variations such as: filtering,[6] orthonormalization,[7] and parallel shooting.[8]

Finite-Difference Methods

In the finite-difference or matrix methods the interval $-1 \leq y \leq 0$ is divided into a uniform (or non-uniform) grid of mesh points and the differential equation is approximated at each mesh point by a difference equation using centered difference approximations to the derivatives. Care is taken to use difference expressions that minimize the truncation error. When the boundary conditions are incorporated, the resulting system of linear equations can be written as a five-banded complex matrix equation

$$[A(\alpha,R) + (c_r + ic_i)B(\alpha)]\Phi = 0.$$

For given α and R this is a standard eigenvalue problem for $c = c_r + ic_i$. Since one usually wants the neutral curve, $c_i = 0$, a double search must be carried out: first find c for given α and R and then vary α until $c_i = 0$. A good estimate for c is usually available (e.g., from a previous R value) so that an efficient numerical eigenvalue method consists of finding the zeros of the determinant $|A - cB|$. This determinant is calculated by reducing the matrix to upper triangular form by Gaussian elimination and then a rootfinder such as that of Aitken, Muller, Newton, or Laguerre is used.[13]

This method was first used on the Orr-Sommerfeld equation by Thomas[9] in 1953 and subsequently by Kurtz,[10,11] Osborne[12] and Gary.[13] Thomas[9] used the method as outlined above without a rootfinder for plane Poiseuille flow and Kurtz[10] studied some boundary layer flows using the above method with Muller's rootfinder. Osborne[12] used a very different inner-outer type iteration scheme and was concerned with the numerical stability of the algorithm. Gary

and Helgason[14] tried to get around the often encountered rootfinder difficulties by transforming the problem to the standard matrix eigenvalue problem $A\Phi = c\Phi$ and then using the QR algorithm to compute the eigenvalues directly.

III. DETERMINATION OF THE VARIABLE MESH

The matrix finite-difference method is used in this study with a non-uniform mesh and a modified eigenvalue search procedure discussed in Section V. It is desirable to have a relatively high density of mesh points in the critical layer and in the viscous layer at the wall where $\phi(y)$ is changing rapidly. Although the mesh spacing might be specified analytically once and for all as in Gary and Helgason[14] or Roberts,[15] the use of an automatically determined and corrected mesh point distribution using the ideas given by Pearson[16,17] appears to be highly flexible and desirable. As in Pearson the mesh point spacing is initially uniform; usually 100 equal intervals in $-1 \leq y \leq 0$ are sufficient. Setting $\phi(0) = 1$ and using an estimate for α, c_r, and R ($c_i = 0$) from Thomas[9] for example, a first approximation to the eigenfunction is calculated by solving the finite difference equations by Gaussian elimination. New mesh points are then inserted between any pair of adjacent mesh points y_i and y_{i+1} for which $|g(y_{i+1}) - g(y_i)|$ exceeds a predetermined limit δ.* The number of such mesh points inserted (uniformly) between y_i and y_{i+1} is approximately equal to $|g_{i+1} - g_i|/\delta$. Using this modified mesh the finite difference equations are solved again, new mesh points inserted, and so on; the process is continued iteratively until $|g_{i+1} - g_i| < \delta$ everywhere. The value of δ is chosen to be a small fraction, ε_1, (usually $\varepsilon_1 = 0.04$ or 0.015) of the computed value of $\max_i\{g_i\} - \min_i\{g_i\}$. Since the insertion of new mesh points may result in a locally abrupt change in interval size, with some consequent loss in the accuracy of the finite-difference approximations, a smoothing process is carried out prior to each new Gaussian elimination sweep. This smoothing process simply consists in replacing each mesh point y_i by a new point y_i' via $y_i' = \frac{1}{2}(y_{i-1}' + y_{i+1})$ for $i = 1,2,3,\ldots$, in sequence. It was found necessary to repeat this smoothing sweep about five times each Gaussian elimination sweep for best results. An example of a non-uniform mesh generated in this way is shown in Figure 3.

*The real and imaginary parts of ϕ are treated as separate real functions denoted collectively in this section by g.

The above paragraph contains a general description of the method used; however two modifications to this basic procedure were found helpful. First, examination of the eigenfunctions revealed a sharp corner at the wall, i.e., ϕ' varies rapidly and requires a dense mesh. The program was modified to examine both the real and imaginary parts of ϕ and ϕ' as above. Higher derivatives could also be examined but this was not found necessary. Secondly, as R becomes larger the viscous layer at the wall and the critical layer crowd toward y = -1 and, since there is no provision for eliminating unnecessary mesh points, the number of mesh points could grow excessively. It was found that the distance from the wall to the critical layer at y_c is a good measure of the width of the dense mesh zone. Thus the routine was modified to permit a compaction of the mesh points toward the wall whenever the estimated c_r was smaller than before. The shifting equations used are*

$$y_i' = y_i + \frac{(y_i + 1)}{(y_c + 1)} (y_c' - y_c) \qquad \text{for } i = 1,2,\ldots,k$$

where k is the largest i such that $y_k < y_c$ and

$$y_i' = y_i + \frac{y_i}{y_c} (y_c' - y_c) \qquad \text{for } i = k+1,\ldots,N-1,$$

where y_c' is the value of y_c at the estimated value of c_r. With these two modifications the routine generated a nearly optimum density of mesh points over the entire range of parameters of interest.

Exactly how this mesh point generating routine is incorporated into the eigenvalue search is somewhat arbitrary. In this study the emphasis was on computing the neutral curve and calculations were started at one value of R and proceeded to a new (usually larger) value of R with c_i set equal to zero. Hence R parameterized the neutral curve and α and c_r were the 'eigenvalues.' For each new value of R, the extrapolated values of α and c_r were used as new estimates and the mesh points from the previous calculation were tested and altered before the eigenvalue search began. Then the mesh point distribution was kept fixed during the eigenvalue search.

---

*The mesh points are numbered with $y_0 \equiv -1$ and $y_N \equiv 0$.

Whenever a calculation was started from a uniform mesh many mesh points were added at first but as R was increased few additional mesh points were needed due to the shifting with y_c. It might appear that the first calculation using a uniform mesh spacing must be performed only at a moderate value of R, but with proper choice of the number of initial uniform points and δ the calculations could be started with a uniform mesh at any Reynolds number up to about 10^9. Details concerning the number of points needed and their density can be found in Section VI and in the figures.

IV. FINITE-DIFFERENCE EQUATIONS

If the non-uniform mesh-point spacing were given by an analytic expression, then the differential equation could be transformed into a new differential equation which could be approximated using finite-difference expressions for uniform spacing. Such an approach has been considered by Roberts[15] and Toomre,[18] however in this study the mesh-point spacing is not so defined and Lagrangian expressions for arbitrary spacing must be used. During the initial phase of this work the Orr-Sommerfeld equation was treated as a single fourth-order equation, then later work used an equivalent second-order system and finally an equivalent first-order system was also tried.* For the purpose of manipulating finite-difference expressions it is more convenient to define $\varepsilon = (i\alpha R)^{-1}$ and write the Orr-Sommerfeld equation as

$$\phi^{iv} + \varepsilon^{-1} f_1(y)\phi'' + \varepsilon^{-1} f_2(y)\phi = 0 \tag{5}$$

where $f_1 \equiv -2\varepsilon\alpha^2 - 1 + c + y^2$ and $f_2 \equiv \varepsilon\alpha^4 + \alpha^2(1-c-y^2) - 2$ and the boundary conditions are $\phi(-1) = \phi'(-1) = \phi'(0) = \phi'''(0) = 0$. An equivalent second-order system is

$$\left.\begin{aligned} &\psi'' + \varepsilon^{-1} f_3(y)\psi - 2\varepsilon^{-1}\phi = 0, \\ &\text{and} \\ &\phi'' - \psi + \alpha^2\phi = 0 \end{aligned}\right\} \tag{6}$$

where $\psi \equiv \phi'' + \alpha^2\phi$ and $f_3 = -\varepsilon\alpha^2 - 1 + c + y^2$ with boundary conditions $\phi(-1) = \phi'(-1) = \phi'(0) = \psi'(0) = 0$. Whereas an equivalent first-order system is expressed as

$$\left.\begin{aligned} \theta' &= -\varepsilon^{-1} f_3\psi + 2\varepsilon^{-1}\phi, & \psi' &= \theta, \\ \chi' &= \psi - \alpha^2\phi, & \phi' &= \chi \end{aligned}\right\} \tag{7}$$

*Prof. H. B. Keller made this suggestion in a private discussion in 1969.

with boundary conditions $\phi(-1) = \chi(-1) = \chi(0) = \theta(0) = 0$. In these equations ϕ, ψ, θ, and χ are all complex functions of y and in the work that follows the finite-difference expressions are complex and the computer programs were written to use complex arithmetic.

As discussed in Hildebrand,[19] for example, denote the mesh points for n odd by y_k, $k = -n,\ldots,o,\ldots,n$, and then the Lagrangian finite difference expression for the r-th derivative of a 2n-th order approximating polynomial is given by

$$\frac{d^r}{dx^r} f(x) \cong \sum_{k=-n}^{k=n} \frac{d^r}{dx^r} (\ell_k(x)) f(x_k),$$

where

$$\ell_k(x) = \frac{(x-x_{-n})\ldots(x-x_{k-1})(x-x_{k+1})\ldots(x-x_n)}{(x_k-x_{-n})\ldots(x_k-x_{k-1})(x_k-x_{k+1})\ldots(x_k-x_n)} .$$

Using this equation the five-point Lagrangian approximation to the fourth derivative evaluated at the center point is found to be

$$\frac{d^4}{dy^4} f(x_o) \cong 24 \sum_{k=-2}^{2} f(x_k)/\pi_k \qquad (8)$$

where $\pi_k = \prod_{\substack{i=-2 \\ i\neq k}}^{2} (x_k - x_i)$. Similarly, the three-point Lagrangian approximation to the second derivative evaluated at the center point is

$$\frac{d^2}{dy^2} f(x_o) \cong \ell''_{-1} f(x_{-1}) + \ell''_o f(x_o) + \ell''_{+1} f(x_{+1}) \qquad (9)$$

where $\ell''_{-1} = \frac{2}{(x_{-1}-x_o)(x_{-1}-x_{+1})}$, $\ell''_o = \frac{2}{(x_o-x_{-1})(x_o-x_{+1})}$, and $\ell''_{+1} = \frac{2}{(x_{+1}-x_{-1})(x_{+1}-x_o)}$. The finite-difference approximations to the fourth-order equation and the pair of second-order equations are obtained by inserting the approximations (8) and (9) into equations (5) and (6) and

evaluating f_1, f_2, and f_3 at $y = y_o$. The first-order system is approximated in such a way that only the values at y_i and y_{i+1} are involved. Define $h = y_{i+1} - y_i$, then the finite-difference equations are given by

$$\frac{1}{h}(\theta_{i+1} - \theta_i) = -\frac{1}{2}\varepsilon^{-1} f_{3,i+\frac{1}{2}}(\psi_{i+1} + \psi_i) + \varepsilon^{-1}(\phi_{i+1} + \phi_i).$$

$$\frac{1}{h}(\psi_{i+1} - \psi_i) = \frac{1}{2}(\theta_{i+1} + \theta_i),$$

$$\frac{1}{h}(\chi_{i+1} - \chi_i) = \frac{1}{2}(\psi_{i+1} + \psi_i) - \frac{1}{2}\alpha^2(\phi_{i+1} + \phi_i),$$

and

$$\frac{1}{h}(\phi_{i+1} - \phi_i) = \frac{1}{2}(\chi_{i+1} + \chi_i)$$

where $f_{3,i+\frac{1}{2}}$ is f_3 evaluated at $y_{i+\frac{1}{2}} = \frac{1}{2}(y_{i+1} + y_i)$.

If the mesh point spacing were uniform, the approximations (8) and (9) would be $O(h^2)$ accurate because of cancellation of the $O(h)$ error terms. In this work the finite-difference approximations to the fourth-order equation and the second-order system are only $O(h)$ accurate where h is the maximum step size over the five points used. However the finite-difference approximations to the first-order system are chosen to extend over only one interval and, therefore, are $O(h^2)$ accurate. This difference in accuracy was strikingly demonstrated in actual calculations. The results of the first-order system for essentially the same mesh as used for the higher-order equations are several orders of magnitude more accurate. Early in this study it was noticed that the second-derivative term in Eq. (5) is multiplied by ε^{-1} and it was felt that using a five-point approximation to the second derivative with $O(h^3)$ error would yield an improvement in accuracy over the three-point approximation. However, the $O(h)$ error term contains the fifth derivative of ϕ, while the $O(h^3)$ error term contains the seventh derivative of ϕ. It should be recalled that one of the solutions of the Orr-Sommerfeld equation is an

exponential with behavior like $\mathrm{Exp}(\varepsilon^{-\frac{1}{2}}y)$ so that $\phi^{(i+1)}/\phi^{(i)} \sim \varepsilon^{-\frac{1}{2}}$. Therefore if $h \sim |\varepsilon^{-\frac{1}{2}}|$, any increase in order of h is cancelled by the increase in the order of differentiation. This was confirmed by actual calculation. It was found that h was about $|\varepsilon^{-\frac{1}{2}}|$ in magnitude in the region near the wall and that the results for both approximations to the second derivative were comparable.

The system of finite-difference equations can be written in matrix form $A(\alpha,c,R)\Phi = 0$. For the fourth-order system the rows are the finite-difference equations centered at $y_1, y_2, \ldots, y_N$ in sequence where $y_o = -1$ and $y_N = 0$. The columns are the coefficients of the unknowns $\Phi_1, \Phi_2, \ldots, \Phi_N$. The boundary conditions are incorporated into this system of equations by setting $\phi(-1) = \Phi_o = 0$, by assuming that $y_o - y_{-1} = y_1 - y_o$ so that $\phi'(-1) = 0$ implies $\Phi_{-1} = \Phi_{+1}$; by assuming that $y_{N+1} - y_N = y_N - y_{N-1}$ so that $\phi'(0) = 0$ implies $\Phi_{N+1} = \Phi_{N-1}$ and finally assuming $y_{N+2} - y_{N+1} = y_{N-1} - y_{N-2}$ so that $\phi'''(0) = 0$ implies $\Phi_{N+2} = \Phi_{N-2}$. The matrix A is an N by N matrix of complex elements with the only nonzero elements along the main diagonal and the two sub- and super-diagonals, i.e., A is five-banded. The set of linear equations approximating the system of second-order equations can also be written as a five-banded complex matrix equation. The rows are the N pairs (ψ'' equation before the ϕ'' equation) of finite- difference equations centered at $y_1, y_2, \ldots, y_N$ in sequence. The columns are the coefficients of the unknowns $\psi_1, \Phi_1, \psi_2, \Phi_2, \ldots, \psi_N, \Phi_N$. The boundary conditions at y = -1 are used to eliminate ψ_o and Φ_o by using $\phi(-1) = \Phi_o = 0$ and by assuming that $y_o - y_{-1} = y_1 - y_o \equiv h$ so that $\phi'(-1) = 0$, which implies $\Phi_{-1} = \Phi_{+1}$, can be combined with a finite difference approximation at y_o to the second equation of (6) to yield $\psi_o = (2/h^2)\Phi_{+1}$. The boundary conditions at y = 0 are used in the same way as with the fourth-order equation to eliminate ψ_{N+1} and Φ_{N+1}. With this ordering the matrix A is a 2N by 2N square five-banded complex matrix.

With careful ordering of the equations and unknowns the set of linear finite-difference equations approximating the first-order system

(7) can be written as a seven-banded complex 4N by 4N matrix equation. The rows are the N sets of equations centered at $y_1, y_2, \ldots, y_N$ in sequence with the equation ordering $\psi' = \ldots$, $\theta' = \ldots$, $\chi' = \ldots$, $\phi' = \ldots$ in each set. The columns are the coefficients of the 4N unknowns, $\theta_o, \psi_o, \theta_1, \psi_1, \Phi_1, \chi_1, \ldots,$ $\theta_{N-1}, \psi_{N-1}, \Phi_{N-1}, \chi_{N-1}, \psi_N, \Phi_N$. The boundary conditions yield $\phi(-1) = \Phi_o = 0$, $\chi(-1) = \chi_o = 0$, $\chi(0) = \chi_N = 0$ and $\theta(0) = \theta_N = 0$. Both storage requirements and computing time would be reduced if one could retain the five-banded structure previously obtained with the fourth-order equation and the second-order system. This can be accomplished by using a 'staggered' difference scheme and careful ordering of the equations and unknowns. The equations containing θ' and χ' would be center-differenced at the y_i points, but the equations containing θ' and ϕ' would be center-differenced at the midpoints between adjacent mesh points. Unfortunately, this system is only O(h) accurate and the advantages of going to a first-order system are lost.

For most of the calculations the second-order system was found to be the best compromise between accuracy and computing time. The calculations using the fourth-order equation were found to be somewhat faster but noticeably less accurate. On the other hand the calculations using the first-order system were about four times slower than the second-order system because there are twice as many equations and one additional subdiagonal band must be transformed to zero by Gaussian elimination. However, about two digits of accuracy could be gained by using the first-order system and this was of great help in the region of the neutral curve in the neighborhood of the kink.

V. SOLUTION OF THE EIGENVALUE PROBLEM

One of the standard methods of solving this general matrix eigenvalue problem, $A(\alpha,R,c_r,c_i)\Phi = 0$, is to use a rootfinder to numerically locate the zeros of the determinant of A, denoted by detA. As with any algorithm that uses a rootfinder routine, the overall method can be very efficient if a good estimate of the location of the zero is available. Since the system of equations is complex, the determinant is also complex and can be used to determine two of the four parameters α, R, c_r, c_i, while the other two are held constant during the eigenvalue search. To obtain the 'neutral curve,' it is convenient to set $c_i = 0$ and calculate the values of α and c_r for a sequence of values of R. Such a sequence of calculations is started from some known results, near R_{min} for example, and then R is incremented to larger values with good estimates of α and c_r obtained by quadratic extrapolation. Another common choice (see Sec. II) would be to assign values of α and R and find $c = c_r + ic_i$; however, this method requires a second iteration to find $c_i = 0$.

To find the zeros of detA, which is a complex-valued nonlinear function of the two real parameters α and c_r, the two-dimensional version of Newton's method is used. This can be written conveniently as a system of two linear equations for the corrections $\Delta\alpha$ and Δc_r:

$$\frac{\partial r}{\partial \alpha}\Delta\alpha + \frac{\partial r}{\partial c_r}\Delta c_r = r^n$$

$$\frac{\partial s}{\partial \alpha}\Delta\alpha + \frac{\partial s}{\partial c_r}\Delta c_r = s^n \qquad (10)$$

where $\Delta\alpha = \alpha^{n+1} - \alpha^n$, $\Delta c_r = c_r^{n+1} - c_r^n$, r is the real part of detA and s is the imaginary part of detA. The partial derivatives of r and s are obtained approximately by computing detA (α^n, c_r^n), detA $(\alpha^n + \delta\alpha, c_r^n)$ and detA $(\alpha^n, c_r^n + \delta c_r)$, and then forming the appropriate ratios. Using good estimates for α and c_r

obtained from previous calculations, the rootfinder usually converged in two to six iterations to the desired accuracy.

The evaluation of the determinant is performed by reducing the matrix A to upper triangular form using Gaussian elimination and then computing the product of the diagonal terms (see Wilkinson,[20] for example). The Gaussian elimination is performed in complex arithmetic in a way that preserves the banded structure of the matrix. The largest element in absolute value below the diagonal in each column is used as the pivot. This 'partial pivoting' may add nonzero elements above the diagonal where zeros existed before, but only in at most the two (in the five-band case) or three (in the seven-band case) superdiagonals above the existing nonzero diagonals. Conceptually the computation of the product of the diagonal terms is a simple operation but when 100 to 1000 or more terms are involved, one invariably has underflow or overflow difficulties even if the numbers are close to one. To avoid this difficulty the determinant is scaled to have a magnitude of unity at the estimated values of α and c_r before the rootfinder iteration begins. The scaling factors are saved and applied throughout the remainder of the rootfinder iterations. When an approximation to the eigenfunction is required either by the mesh generating and testing routine or for final results, the value of $\phi(0)$ is set equal to unity and then the resulting set of nonhomogeneous equations is solved by back substitution.

This technique of finding the eigenvalues, α and c_r, by locating the zeros of the determinant worked reasonably well to the three digit accuracy required for the graphical results. However in the region of the neutral curve around the kink, the method was inadequate. The difficulty was traced to the fact that the numerically computed determinant is not very sensitive to the choice of α and c_r, i.e., a fairly large change in α or c_r made only a small change in the value of detA. Previous work using this method (see Sec. II) was formulated in such a way that $c = c_r + ic_i$ is the eigenvalue rather than α and c_r. It may be

that c is a better eigenvalue even though a double search is required. Thomas[9] experienced the opposite difficulty (instability) when he performed the Gaussian elimination starting at the center $y = 0$ and working toward the wall $y = -1$. However, when the Gaussian elimination was started at the wall--as done here--he was able to find the roots.

Improved Eigenvalue Search

Because the determinant evaluation method did not yield wholly satisfactory results an alternative method of finding the eigenvalues was sought. The following method has been found to be very successful. Instead of finding the zeros of detA, $\phi(0)$ is set equal to unity and one of the boundary conditions is left unsatisfied when the finite-difference equations are set up. The Newton rootfinder is used to find the parameter values such that the unsatisfied boundary condition is correct. In this study the boundary condition $\phi(-1) = 0$ was not satisfied initially and α and c_r were sought so that $\phi(-1) = 0$ is satisfied. The resulting set of linear equations is nonhomogeneous, i.e., $A\Phi = b$, and can be solved for given values of α and c_r by Gaussian elimination starting at $y = -1$ and back substitution to get the value of Φ at $y = -1$. The matrix A is still five-banded (seven bands in the first-order system case) but the unknowns are now $\Phi_0, \Phi_1, \ldots, \Phi_{N-1}$ and there is only one nonzero subdiagonal band (two subdiagonals for the first-order system) to be set to zero by the Gaussian elimination. This method is highly reliable and one can obtain four to six digit accuracy along the entire neutral curve.

Another distinct advantage of this method is that the partial derivatives needed by the Newton rootfinder can be calculated by solving the differential equations satisfied by $\frac{\partial \phi}{\partial \alpha}$ and $\frac{\partial \phi}{\partial c_r}$. Let L_{OS} denote the Orr-Sommerfeld operator

$$\frac{d^4}{dy^4} - 2\alpha^2 \frac{d^2}{dy^2} + \alpha^4 - i\alpha R\left[(1 - y^2 - c)\left(\frac{d^2}{dy^2} - \alpha^2\right) + 2\right]$$

and let $\bar{\phi} \equiv \frac{\partial \phi}{\partial \alpha}$ and $\hat{\phi} \equiv \frac{\partial \phi}{\partial c_r}$. For given values of α, $c = c_r + ic_i$, and R, the complex functions ϕ, $\bar{\phi}$ and $\hat{\phi}$ are given by the solutions of the following three problems:

$$\text{(i)} \quad L_{OS}\phi = 0,\ \phi'(-1) = 0,\ \phi(0) = 1,\ \phi'(0) = \phi'''(0) = 0,$$

$$\text{(ii)} \quad L_{OS}\bar{\phi} = \bar{f};\ \bar{\phi}'(-1) = 0,\ \bar{\phi}(0) = \bar{\phi}'(0) = \bar{\phi}'''(0) = 0,$$

$$\text{where } \bar{f} = 4\alpha\phi'' - 4\alpha^3\phi + iR[(1-y^2-c)(\phi''-3\alpha^2\phi) + 2\phi]$$

$$\text{(iii)} \quad L_{OS}\hat{\phi} = \hat{f};\ \hat{\phi}'(-1) = 0,\ \hat{\phi}(0) = \hat{\phi}'(0) = \hat{\phi}'''(0) = 0,$$

$$\text{where } \hat{f} = -i\alpha R(\phi'' - \alpha^2\phi).$$

Problems (ii) and (iii) are referred to as variational problems by Keller.[8] The finite-difference approximations to these three problems yield three systems of linear equations $A\Phi = b$, $A\bar{\Phi} = \bar{b}$, $A\hat{\Phi} = \hat{b}$ where A is the same matrix in all three problems. The unknown vectors Φ, $\bar{\Phi}$, $\hat{\Phi}$ are the finite-difference approximations to ϕ, $\bar{\phi}$, $\hat{\phi}$ respectively, b is the nonhomogeneous right hand side due to the normalization condition $\phi(0) = 1$ and $\bar{b}$ and $\hat{b}$ are finite-difference approximations of $\bar{f}$ and $\hat{f}$. These three problems can be solved together by transforming A to upper triangular form, solving for Φ and next computing $\bar{b}$ and $\hat{b}$. Then the required values $\bar{\Phi}(-1)$ and $\hat{\Phi}(-1)$ can be calculated by transforming $\bar{b}$ and $\hat{b}$ with multipliers saved from the previous triangularization and then back substitution. It is assumed that the nonuniform mesh spacing appropriate to ϕ is also appropriate for $\bar{\phi}$ and $\hat{\phi}$.

The author is not aware of any extensive development in the numerical analysis literature of the technique of partially satisfying the boundary conditions of a high-order two-point boundary-value problem and using the unsatisfied boundary condition as a characteristic equation to determine the eigenvalue. Nevertheless, it would appear that the idea has wide appeal because the often tricky and inaccurate calculation of a determinant is replaced by

the finding of the solution to a set of linear equations by well established and reliable methods. The use of this technique here was motivated by experience with solving the eigenvalue problem when asymptotic approximations are used.[4,21] Having found asymptotic approximations to four independent solutions of the Orr-Sommerfeld equation, the eigenvalue problem is solved by first imposing a normalization condition somewhere in $-1 \leq y \leq 0$ (namely, the non-singular inviscid solution ϕ_1 is set equal to unity at $y = y_c$). Next a linear combination of the inviscid solutions is required to satisfy the boundary conditions at $y = 0$ (ϕ_3 is exponentially small at $y = 0$ and ϕ_4 is rejected). Finally the 'characteristic equation' used to find the eigenvalues is the condition for satisfying the boundary conditions at $y = -1$. This characteristic equation is solved using a Newton rootfinder. Reliable and accurate results were easily obtained. A closely related technique was discussed in a paper by Reynolds and Potter[22] who used a filtered shooting scheme to construct a solution for given α, R and c, which satisfied the central boundary conditions and one of the wall conditions. A Newton rootfinder was then used to adjust two of the parameters until the second wall condition was satisfied.

It is of interest to note how this improved eigenvalue search procedure would be used in the case of boundary-layer velocity profiles. The Orr-Sommerfeld equation (2) still applies but now the region of interest extends from $y = 0$ to $y \to +\infty$. The boundary con- The boundary conditions are $\phi(0) = \phi'(0) = 0$ and $\phi \sim \exp(-\alpha y)$ as $y \to \infty$. In numerical studies[10,12] one usually chooses some point, y_b, outside the boundary layer at which Eq. (2) can be simplified and solved analytically and then the numerical integration extends from $y = 0$ to $y = y_b$. To apply the method discussed here, the boundary condition $\phi(0) = 0$ would be temporarily relaxed. The Gaussian elimination would be carried out from $y = 0$ to $y = y_b$ with a normalization condition on ϕ at y_b, and then back substitution would yield $\phi(0)$ as the characteristic function to be used with the Newton rootfinder.

VI. RESULTS AND CONCLUSIONS

The aim of this study is to explore the use of an automatically determined variable mesh in the numerical solution of the Orr-Sommerfeld equation for plane Poiseuille flow. It was found necessary to modify the usual matrix finite-difference eigenvalue search procedure. Accurate results are obtained which extend far into the range where asymptotic results for large Reynolds number apply. Familiarity with the asymptotic methods and results was found very useful in developing an efficient numerical scheme. All calculations were performed on a CDC 3600 computer in single precision arithmetic (10 significant digits) using the machine facilities for complex arithmetic when needed. All results presented in the figures - except for the kink - were calculated using the second-order system (6) with the improved eigenvalue search technique and an initial uniform mesh of 100 points with the mesh testing parameter ε_1 equal to .04.

The overall neutral curve is shown in Figure 1. This figure was taken from Reid[4] and on the scale of the figure the difference between the asymptotic and numerical results can not be discerned. Figure 2 displays the neutral curve around the minimum value of R and shows a comparison of several different studies. The present numerical calculations in this region required about 170 mesh points and about 12 seconds of computing per point on the neutral curve. Three eigenfunctions at selected values of R are shown in Figures 5 and 6. These eigenfunctions are compared to the inviscid eigenfunction for $R = \infty$ given by $\phi_\infty = 1 - y^2$.* It can be seen that except for near the wall and the critical point y_c, the eigenfunctions are close to the ϕ_∞ eigenfunction.

In Figure 4 the neutral curves are shown using 100, 200, and 500 uniform points. These calculations were performed using the improved eigenvalue search procedure. Even though the

*In the limit $R = \infty$, $\alpha = 0$ and $c = 0$; then Eq. (4) reduces to $\phi''/\phi = U''/U$ which by inspection has the solution $\phi(y) = U(y) = 1-y^2$.

finite-difference approximations (8) and (9) with a uniform mesh are not as accurate as those previously used,[9,10,12,14] the results suggest that the uniform mesh calculations are reasonably accurate for plane Poiseuille flow up to a Reynolds number of about 10^5. A typical case of the non-uniform mesh spacing generated using the method discussed in Section III is shown in Figure 3. The effect of the smoothing of the mesh point spacing can be seen. This smoothing was found to be very important; without it the eigenvalues were highly dependent upon the choice of mesh spacing even in the case of the first-order system. The method used in this study is very general and worked quite well, however after having calculated several examples of this class of problem it may be possible to preassign the mesh points with confidence. From Figure 3 and many other similar results it can be concluded that this problem requires two uniform mesh regions with a transition between (perhaps a cubic polynomial). The difficulty is that the location, extent and size of the fine mesh region is not precisely known. However, these results suggest that the fine mesh should obviously be next to the wall at $y = -1$, that a multiple of $(y_c + 1)$ may give a good estimate of the extent of the fine mesh and that a mesh size between $|\alpha R|^{-1}$ and $|\alpha R|^{-\frac{1}{2}}$ would be appropriate.

In order to get some idea of the limitations of the method described in this report, the calculations were carried out to very large Reynolds numbers until they failed. A very useful test of the accuracy of the results is to compare them to the asymptotes to the neutral curve given by the following:[4]

$$\text{Upper branch,} \quad R^{1/3} = 8.44(\alpha^2)^{-11/16},$$

$$\text{Lower branch,} \quad R^{1/3} = 5.96(\alpha^2)^{-7/6}.$$

The following results were calculated in single precision using the first-order system of equations and starting at $R = 10^8$ with 100 uniform points and with $\varepsilon_1 = 0.04$. Along the upper branch the calculations went to $R = 10^{14}$ at which point the results were very close to the asymptote values but the accuracy of the characteristic

function $\phi(0)$ was no longer sufficient to find an accurate root. Along the lower branch the calculations proceeded very accurately to about $R = 10^{12}$ at which point the numerical results began to diverge from the asymptote in a manner similar to that shown in Figure 4 for the 100 uniform point case. Generally the number of mesh points was less than 400 and the smallest automatically generated mesh point spacing was about 0.1 to 0.01 times $(\alpha R)^{-\frac{1}{2}}$ and many orders of magnitude larger than $(\alpha R)^{-1}$.

The kink in the neutral curve

The kink in the neutral curve is a puzzling detail at large Reynolds number that appeared in earlier work using asymptotic methods.[4,21] It was conjectured that the kink was due to a deficiency in the asymptotic approximations and might disappear if a higher-order-accurate theory were developed. In the most commonly used version of the asymptotic theory the kink can be traced to the loop in the graph of a complex function, called the Tietjen's function, that occurs in the characteristic equation. The Tietjen's function, F(z), is the ratio of certain integrals in the complex plane of the Airy function, Ai(ξ), (see e.g., Reid[4]):

$$F(z) = \frac{\int_{\infty_1}^{\xi_1} d\xi \int_{\infty_1}^{\xi_1} \mathrm{Ai}(\xi)\,d\xi}{\xi_1 \int_{\infty_1}^{\xi} \mathrm{Ai}(\xi)\,d\xi}$$

where $\xi_1 = ze^{-5\pi i/6}$ and $z = (-2\alpha R y_c)^{1/3}(1+y_c)$.

The results using the numerical method in this report show that the kink is in fact a feature of the eigenvalues of the Orr-Sommerfeld equation. An enlarged plot of the kink region of the neutral curve including both asymptotic and numerical results is shown in Figures 7 and 8. Three eigenfunctions at selected points along the neutral curve

are shown in Figure 9. It should be noted that the eigenfunctions do not change qualitatively as one passes through the kink region. These results were obtained using the first-order system of equations, single precision arithmetic (10 digit), and about 400 mesh points. The calculation can be started with a uniform mesh (100 points) both at an R value less than the kink region - working forward in R through the kink - and also starting at a large R value and working back through the kink. The difference in the results is not discernable on the scale used in Figures 7 and 8. It is interesting to note that the asymptotic calculations required ½sec per point on the curve while the slow (but accurate) first order finite-difference calculation required about 40 seconds per point.

The importance of the kink should not be overemphasized since it is unlikely that it has any physical significance since - at least for plane Poiseuille flow - it occurs at a Reynolds number too large for the linear theory to be relevant. However, these calculations are difficult and led to several significant improvements in the numerical method. Although early calculations in this study suggested that the kink existed, each reasonable numerical improvement in the method made the calculations more accurate and more reliable. These improvements include (i) the improved eigenvalue search discussed in Section V, (ii) the use of the more accurate first-order system, and (iii) a change in the eigenvalue parameterization. As can be seen in Figures 1 and 7, the neutral curve is multiple valued for fixed constant values of α or R. The calculation can proceed much more smoothly if a single monotonic variable were available to parameterize the entire neutral curve. In the asymptotic theory z, defined above, is just such a parameter. It tends to 2.30 as R increases along the lower branch of the neutral curve and tends to infinity along the upper branch with values in the neighborhood of 5.5 at the kink. With this in mind the eigenvalue search was modified to include the option of stepping the calculations at fixed values of z and finding α and c_r with $c_i = 0$. With this modification the kink in the neutral curve could be traced out without any difficulty with the rootfinder due to closely spaced multiple roots.

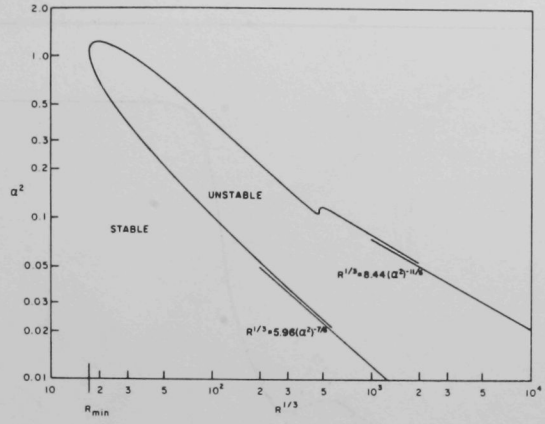

Fig. 1. The Curve of Neutral Stability for Plane Poiseuille Flow (adapted from reference 4).

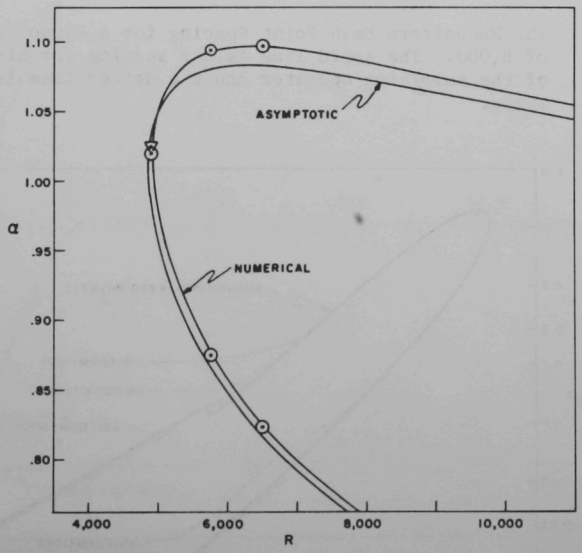

Fig. 2. The Neutral Curve near the Minimum Reynolds Number. The points enclosed by circles are from Reynolds & Potter[22] and the point surrounded by a triangle is from Thomas.[9]

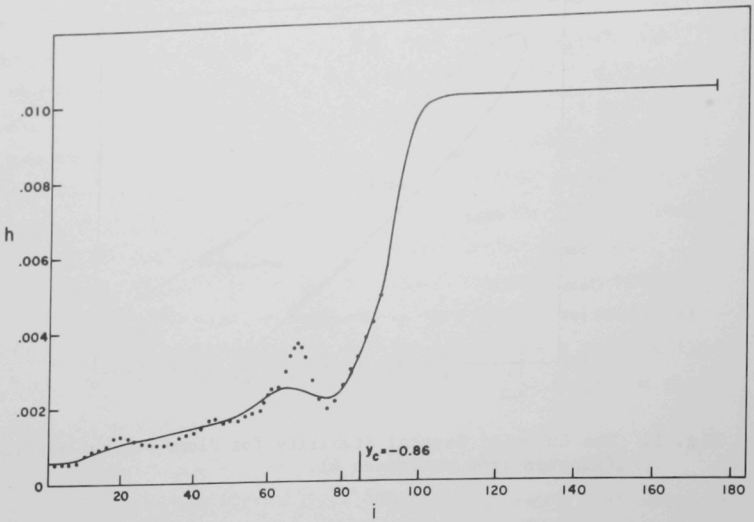

Fig. 3. The Nonuniform Mesh Point Spacing for a Reynolds Number of 8,000. The solid line is the spacing for nine sweeps of the smoothing operator and the dotted line is for one sweep.

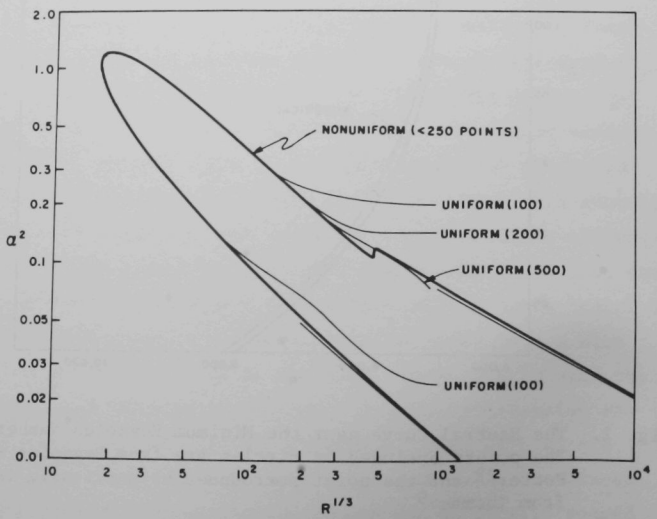

Fig. 4. Curves of Neutral Stability Using Various Uniform Point Distributions.

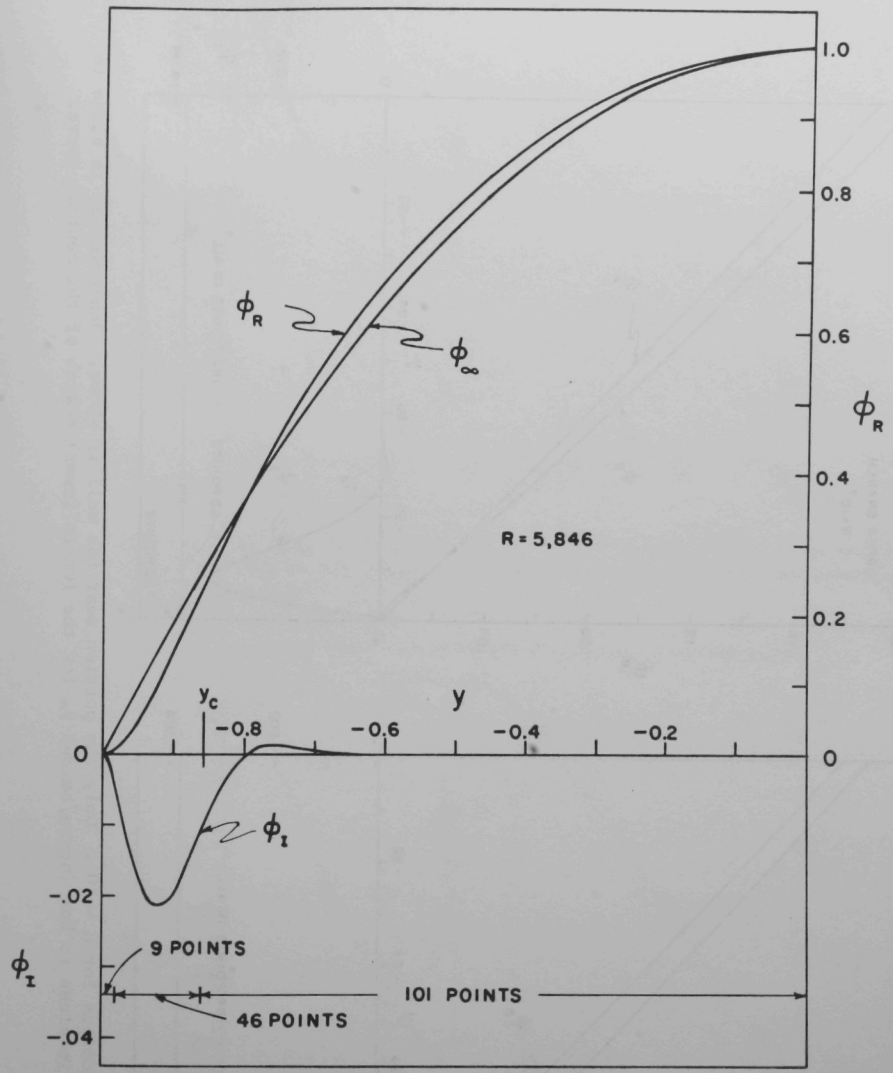

Fig. 5. The Eigenfunction for R = 5,846 (near R_{min}).

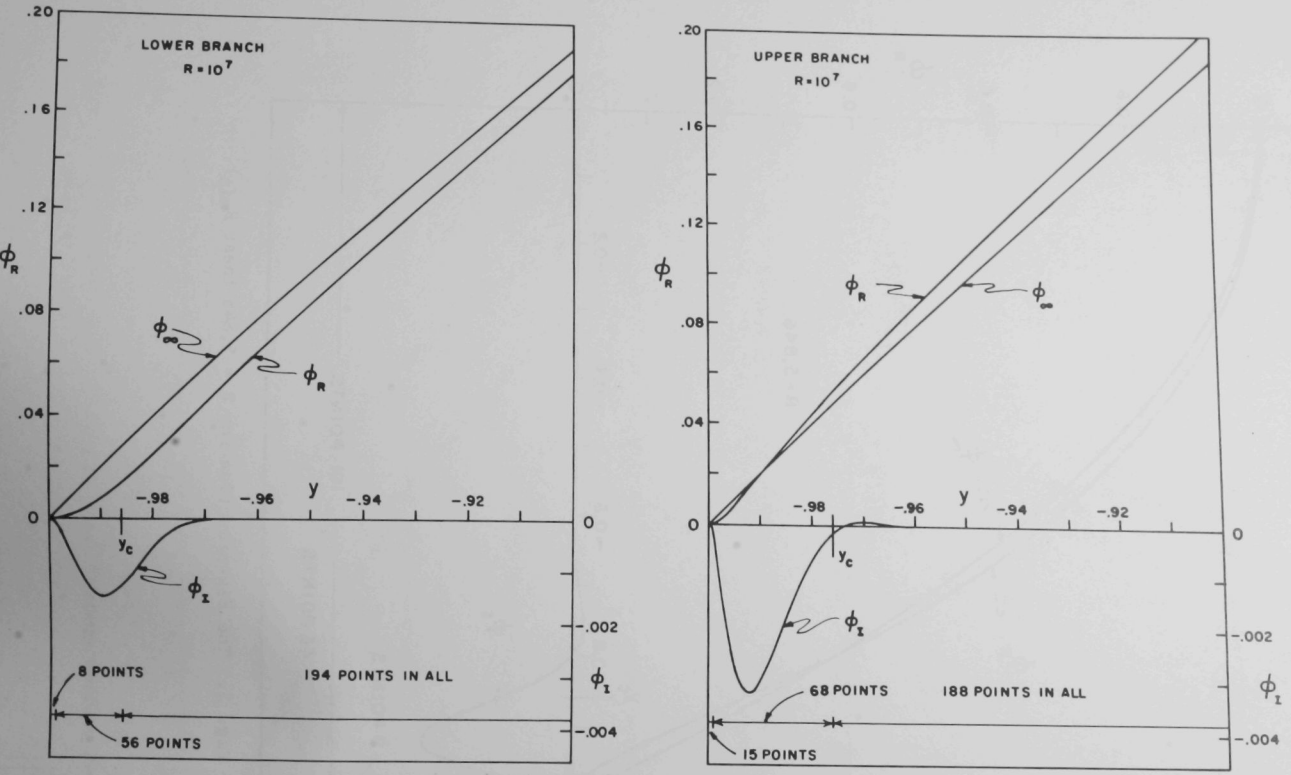

Fig. 6. The Eigenfunctions for R = 10^7. Only the portion near the wall is shown. Otherwise ϕ_I is close to zero and ϕ_R is close to but (above/below) ϕ_∞ for the (upper/lower) branch of the neutral curve.

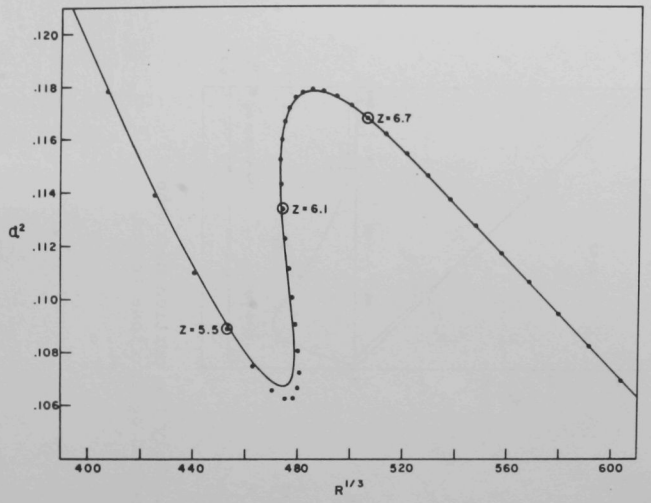

Fig. 7. The Kink in the Neutral Curve (α^2 versus $R^{1/3}$). The solid line is the asymptotic result and the dots are the numerical results.

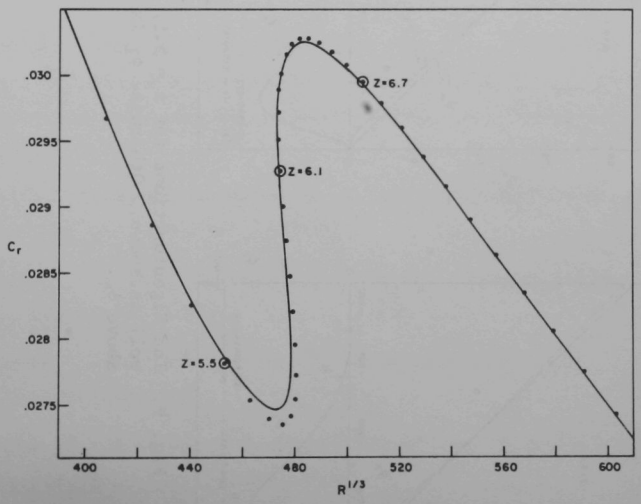

Fig. 8. The Kink in the Neutral Curve (c_r versus $R^{1/3}$). The solid line is the asymptotic result and the dots are the numerical results.

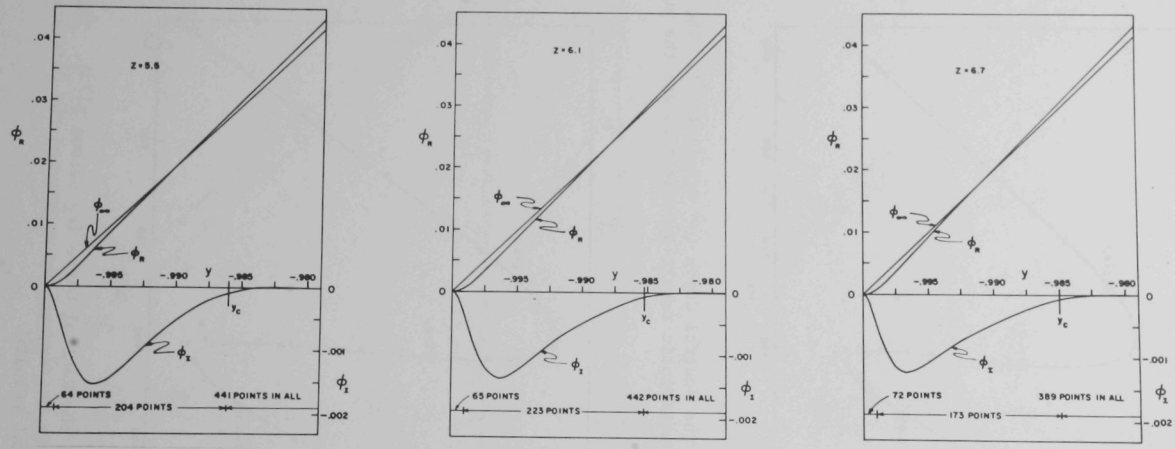

Fig. 9. The Eigenfunctions for z = 5.5, 6.1 and 6.7. Only the portion near the wall is shown. Otherwise ϕ_I is close to zero and ϕ_R is close to but above ϕ_∞.

VII. REFERENCES

1. C. C. Lin, The theory of hydrodynamic stability, Cambridge University Press, 1955.

2. J. T. Stuart, Hydrodynamic stability, Fluid Motion Memoirs: Laminar Boundary Layers (Ed.: L. Rosenhead), 492-579, Oxford University Press, 1963.

3. S. F. Shen, Stability of laminar flows, Theory of laminar flows (Ed.: F. K. Moore), 719-853, Princeton University Press, 1964.

4. W. H. Reid, The stability of parallel flows, Basic developments in fluid dynamics (Ed.: M. Holt), 249-307, Academic Press, New York, 1965.

5. P. R. Nachtsheim, An initial value method for the numerical treatment of the Orr-Sommerfeld equation for the case of plane Poiseuille flow, NASA TN D-2414, Lewis Research Center - N.A.S.A., 1964.

6. R. E. Kaplan, Solution of Orr-Sommerfeld equation for laminar boundary layer flow over compliant boundaries, ASRL-TR-116-1, Cambridge Aeroelastic and Structures Research Lab., Mass. Inst. Tech., 1964.

7. S. D. Conte, The numerical solution of linear boundary value problems, SIAM Rev. 8 (1966), 309-321.

8. H. B. Keller, Numerical methods for two-point boundary-value problems, Blaisdell, Waltham (Mass.), 1968.

9. L. H. Thomas, The stability of plane Poiseuille flow, Phys. Rev. 91 (1953), 780-783.

10. E. F. Kurtz Jr., A study of the stability of laminar parallel flows, Thesis, Mass. Inst. Tech., 1961.

11. E. F. Kurtz Jr. and S. H. Crandall, Computer-aided analysis of hydrodynamic stability, J. Math. Phys. 41 (1962), 264-279.

12. M. R. Osborne, Numerical methods for hydrodynamic stability problems, SIAM J. Appl. Math. 15 (1967), 539-557.

13. J. Gary, Computing eigenvalues of ordinary differential equations by finite differences, Math. Comp. 19 (1965), 365-379.

14. J. Gary and R. Helgason, A matrix method for ordinary differential eigenvalue problems, J. Comp. Phys. 5 (1970), 169-187.

15. G. O. Roberts, Computational meshes for boundary layer problems, Proc. Second International Conf. Num. Methods Fluid Dynamics, Berkeley (Ed.: M. Holt), Springer-Verlag, Berlin, 1971, 171-177.

16. C. E. Pearson, On a differential equation of boundary layer type, J. Math. Phys. 47 (1968), 134-154.

17. C. E. Pearson, On non-linear ordinary differential equations of boundary layer type, J. Math. Phys. 47 (1968), 351-358.

18. J. Toomre, Personal communication (1971).

19. F. B. Hildebrand, Introduction to numerical analysis, McGraw-Hill, New York, 1956.

20. J. H. Wilkinson, The algebraic eigenvalue problem, Oxford University Press, 1965.

21. T. H. Hughes and W. H. Reid, The stability of spiral flow between rotating cylinders, Phil. Trans., Roy. Soc. London. #1135, 263 (1968), 57-91.

22. W. C. Reynolds and M. C. Potter, Finite-amplitude instability of parallel shear flows, J. Fluid Mech. 27 (1967), 465-492.